

DESIGN, CONSTRUCTION, AND CALIBRATION  
OF A SMALL SUBSONIC WIND TUNNEL

by *GLJ*

WILLIAM LEE LEWIS

B. S., Kansas State University, 1969

---

A THESIS

submitted in partial fulfillment of the

requirements for the degree

MASTER OF SCIENCE

Department of Mechanical Engineering

KANSAS STATE UNIVERSITY  
Manhattan, Kansas

1970

Approved by:

*Robert L. Gordon*  
Major Professor

LD  
2668  
T4  
1970  
L48  
C.2

## TABLE OF CONTENTS

Chapter	Page
I. INTRODUCTION. . . . .	1
II. SYSTEM ANALYSIS . . . . .	3
Test Section Loss. . . . .	5
Contraction Section Loss . . . . .	6
Settling Chamber Loss. . . . .	7
First Honeycomb Section Loss . . . . .	8
Diffuser Loss. . . . .	8
Second Honeycomb Section Loss. . . . .	10
Fan Exit Loss. . . . .	11
Total Loss and Summary . . . . .	11
III. SYSTEM DETAILS. . . . .	15
Inlet. . . . .	15
Settling Chamber and Filter. . . . .	15
Contraction Section. . . . .	18
Test Section . . . . .	19
Diffuser . . . . .	19
Fan and Flow Regulator . . . . .	22
IV. CHARACTERISTIC RESULTS. . . . .	23
V. SUMMARY . . . . .	34
REFERENCES. . . . .	35
APPENDICES. . . . .	36
Appendix A . . . . .	37
Appendix B . . . . .	40
ACKNOWLEDGEMENTS. . . . .	42

**THIS BOOK  
CONTAINS  
NUMEROUS PAGES  
WITH DIAGRAMS  
THAT ARE CROOKED  
COMPARED TO THE  
REST OF THE  
INFORMATION ON  
THE PAGE.**

**THIS IS AS  
RECEIVED FROM  
CUSTOMER.**

## LIST OF TABLES

Table	Page
I. Summation of Energy Loss Coefficients . . . . .	12
II. Contraction Co-ordinates for Two-Dimensional Contraction, Ratio 4.23 to 1.00. . . . .	20

## LIST OF FIGURES

Figure	Page
1. Pressure-Volume Flow for 12 Inch Wind Tunnel and Fan. . . . .	14
2. 12 Inch Wind Tunnel . . . . .	16
3. Detail of Inlet, Settling Chamber and Filter, and Contraction Sections. . . . .	17
4. Test Section Detail . . . . .	21
5. Cross-Sectional Velocity Profile 7 1/2 Inches From Start of Test Section at a Test Section Velocity of 139 ft/sec . . . . .	26
6. Cross-Sectional Velocity Profile 28 1/2 Inches From Start of Test Section at a Test Section Velocity of 140 ft/sec . . . . .	27
7. Cross-Sectional Velocity Profile 46 1/2 Inches From Start of Test Section at a Test Section Velocity of 142 ft/sec . . . . .	28
8. Cross-Sectional Velocity Profile 7 1/2 Inches From Start of Test Section at a Test Section Velocity of 47 ft/sec. . . . .	29
9. Cross-Sectional Velocity Profile 28 1/2 Inches From Start of Test Section at a Test Section Velocity of 48 ft/sec. . . . .	30
10. Cross-Sectional Velocity Profile 46 1/2 Inches From Start of Test Section at a Test Section Velocity of 48 ft/sec. . . . .	31
11. Cross-Sectional Velocity Profile 7 1/2 Inches From Start of Test Section at a Test Section Velocity of 92 ft/sec. . . . .	32



## CHAPTER I

### INTRODUCTION

The purpose of this thesis was to design, build, and test a small subsonic wind tunnel that could be used in class laboratory work, aerodynamic experiments, and convection heat and mass transfer experiments. Although not a monumental task, the problem was to build a tunnel with a minimum test section velocity of 100 ft/sec, to include a test section of sufficient size that conveniently sized experiments may be carried out, and to make use of the unused 10 horsepower centrifugal fan that was available in the Mechanical Engineering Department.

The design method was to use proven designs as much as possible and to use proven design procedures for the remainder. It may seem that this design method prevents imagination in the design of the wind tunnel. However, this is not the case. Several special features were incorporated into this wind tunnel without violating proven design procedures.

Special features of this wind tunnel include slots in the settling chamber for screens for turbulence level control, a flow regulator to adjust the rate of flow through the test section, and casters to make the whole tunnel portable. Another important feature of the wind tunnel is the versatile test section. The test section contains two parts that are easily separated and removed. In this way either one or both parts or even a different test section may be used. The test sections are also easily

disassembled, allowing plexiglass sides and/or a floor with experimental apparatus to be installed. Also the test section is supported only at the ends; thus there are no obstructions that would get in the way of experimental equipment attached to the test section.

After design and construction were completed the system was tested to determine velocity ranges and velocity uniformity. Stevenson[1] stated that a velocity deviation of  $\pm 2.0\%$  or less was sufficient for a wind tunnel of this nature. Thus a velocity deviation of  $\pm 2.0\%$  or less from centerline velocity was the goal for this tunnel.

## CHAPTER II

### SYSTEM ANALYSIS

After searching the available literature, it was found that to match a given size test section and given test section velocity to a particular fan an energy loss analysis must be made. This energy loss across the wind tunnel is compared to the characteristic fan curve to find out if the fan is capable of producing the stated test section velocity for the particular size test section. It was decided that a test section 12 inches square and 60 inches long would be an appropriate size. Thus the problem was to see if the given fan could produce a velocity of at least 100 ft/sec through a 12 inch by 12 inch by 60 inch test section.

Due to skin friction, expansion and contraction of the air, screens, and honeycombs, there are energy losses as the air goes through the tunnel. One way to find the amount of these losses is to find the loss in each section of the tunnel separately, and then to sum them[2]. To do this, first define  $K = \Delta P/q$  where  $K$  is the coefficient of loss,  $\Delta P$  is the static pressure drop, and  $q$  is the dynamic head. Redefining the coefficient of loss ( $K$ ) of any section in terms of the dynamic head in the test section ( $q_o$ ), a new loss coefficient,  $K_o$ , is established.

$$K_o = (\Delta P/q_o) = (\Delta P/q)(q/q_o) = K(q/q_o) \quad (1)$$

where  $K_o$  is the coefficient of loss in any section based on  $q_o$ , the dynamic head in the test section. Since the dynamic head varies inversely with the square of the cross-sectional area of the tunnel,

$$K_o = K(A_o/A)^2 \quad (2)$$

where  $A_o$  is the cross-sectional area of the test section and  $A$  is the cross-sectional area of the local section. Then, by definition of the energy loss, the energy loss in each section is

$$\Delta E = K(\dot{m}V^2/2) = K(\rho AV^3/2) \quad (3)$$

where  $\dot{m}$  is the mass flow rate,  $V$  is the fluid velocity, and  $\rho$  is the fluid density. Since the cross-sectional area varies inversely with the velocity,

$$A/A_o = V_o/V$$

or

$$V = A_o V_o / A. \quad (4)$$

Substituting equation (4) into equation (3) gives

$$\Delta E = K\rho A(A_o V_o / A)^3/2 = K\rho A_o V_o^3(A_o/A)^2/2 \quad (5)$$

and substituting equation (2) into equation (5) leaves

$$\Delta E = K_o \rho A V_o^3/2. \quad (6)$$

Now define the Energy Ratio,  $E. R. _t$ , as

$$E. R. _t = \text{Test Section Flow Energy/Circuit Energy Losses} = (\rho A_o V_o^3/2) / (\sum K_o \rho A_o V_o^3/2) = 1/\sum K_o. \quad (7)$$

Thus the Energy Ratio may be found by computing the coefficient of loss of each section as a function of  $K_o$ , summing the  $K_o$ 's, and taking the inverse.

The sections in which the losses are computed include:

1. The test section.
2. The contraction section which is immediately upstream of the test section.
3. The settling chamber which precedes the contraction section.
4. The honeycomb which is immediately upstream of the settling chamber.
5. The diffuser which is immediately downstream of the test section.

6. A honeycomb preceeding the fan and immediately downstream of the diffuser.
7. The fan.

#### Test Section Loss

In the test section the pressure drop in a length of section 'L' is

$$\Delta P/L = f\rho V^2/2D. \quad (8)$$

Since

$$K = \Delta P/q = \Delta P/\rho V^2/2$$

can be substituted into equation (8), then

$$K = fL/D_o = K_o \quad (9)$$

where  $K = K_o$ ,  $L = L_o$  is the length of the test section,  $D = D_o$  is the hydraulic diameter of the test section, and  $f$  is the skin friction coefficient(friction factor). The hydraulic diameter,  $D$ , is expressed as

$$D = 4A/P$$

where  $A$  is the cross-sectional area and  $P$  is the perimeter of the duct.

Thus the hydraulic diameter in this case is

$$D = 4(1 \text{ ft})(1 \text{ ft})/4(1 \text{ ft}) = 1 \text{ ft} = D_o.$$

To find  $K_o$ , the friction factor must be found. To find the friction factor the Reynolds Number, and thus the velocity and viscosity, must be known. Assuming the 100 ft/sec for the velocity at a temperature of 60° F, the air has a kinematic viscosity,  $\nu$ , of approximately  $1.6 \times 10^{-4} \text{ ft}^2/\text{sec}$ .

The Reynolds Number,  $Re$ , is

$$Re = V(D_o/\nu) = 100(1/1.6 \times 10^{-4}) = 6.25 \times 10^5$$

and the friction factor from the Moody chart is approximately

$$f = 0.0125.$$

Now the coefficient of loss in the test section can be found. Substituting the above friction factor and hydraulic diameter along with the length of the test section (5 ft) gives

$$K_o = fL/D_o = 0.0125(5 \text{ ft}/1 \text{ ft}) = 0.0630.$$

#### Contraction Section Loss

The contraction for a 12 inch tunnel would be a two-dimensional contraction, 38 inches long and a 4.23 to 1.00 contraction ratio(51x12 inch inlet and 12x12 inch exit). The design details of the contraction may be found in the next chapter.

The contraction losses may be derived by starting with the expression for the pressure drop in the contraction;

$$\Delta P = \int_0^{L_c} f(\rho V^2/2) dL/D \quad (10)$$

where  $L_c$  is the length of the contraction. An integration is required since both the speed and Reynolds Number vary throughout the contraction. However, Pope and Harper[3] give an approximate empirical formula, using the justification that the contraction loss seldom exceeds 5 per cent of the total loss.

This formula is

$$K_o = 0.32 f_{ave} L_c/D_o$$

where  $f_{ave}$  is the mean friction factor. Now that an expression for  $K_o$  has been determined, the next problem is to determine a friction factor.

Since the hydraulic diameter, and therefore the Reynolds Number, changes through the contraction, the friction factor will also change. Thus an average or mean friction factor must be found. Assuming a linear relation between the friction factor at the inlet(which would be the same as in the settling chamber and is derived in the next section, Settling Chamber Loss)

and the friction factor at the exit(which would be the same as in the test section), the average between the two would be the average friction factor of the contraction section. Thus the average friction factor of the contraction is

$$f = (0.0126 + 0.0146)/2 = 0.0136.$$

With this information  $K_o$  becomes

$$K_o = 0.32fL_c/D_o = 0.32(0.0136)(38/12)/1 = 0.0138.$$

#### Settling Chamber Loss

The energy loss in the settling chamber is due to friction only.

The losses would be computed like in the test section. Referring to equation (9),

$$K = f(L/D)$$

where  $L$  is the length of the settling chamber and  $D$  is the hydraulic diameter of the settling chamber. The length of the settling chamber is 1.75 feet, and the hydraulic diameter is

$$D = 4A/P = 4(4.25)\text{ft}^2/10.5 \text{ ft} = 1.62 \text{ ft}.$$

According to the law of conservation of mass the velocity through the settling chamber would be

$$V_{sc} = A_o V_o / A_{sc} = (1)(100)\text{ft}^2 \cdot \text{ft} / 4.25\text{ft}^2 \cdot \text{sec} = 23.5 \text{ ft/sec}$$

where the subscript "sc" denotes "settling chamber". The Reynolds Number would be

$$Re_{sc} = V_{sc} D_{sc} / \nu = (23.5)(1.62) / 1.6 \times 10^{-4} = 2.38 \times 10^5$$

which corresponds to a friction factor of approximately

$$f = 0.0146$$

from the Moody chart. Substituting this information into equation (9) gives

$$K = f(L_{sc}/D_{sc}) = 0.0146(1.75/1.62) = 0.0158,$$

hence

$$K_o = K(A_o/A)^2 = 0.0158(1/4.25)^2 = 0.000875.$$

#### First Honeycomb Section Loss

The first honeycomb is upstream of the settling chamber. Although a 1 inch filter is used in place of the first honeycomb in the actual tunnel, a hexagonal honeycomb with length to diameter ratio of 6.0 was used in the original energy loss analysis. The honeycomb losses are usually found by assuming a suitable value for the loss coefficient. Pope[2] recommends a K of 0.20 for hexagonal type honeycombs with a length to diameter ratio of 6.0. With this value for the loss coefficient,  $K_o$ , becomes

$$K_o = K(A_o/A_s)^2 = (0.20)(1/4.25)^2 = 0.0111$$

where  $A_o$  is the cross-sectional area of the test section and  $A_s$  equals the cross-sectional area of the settling chamber and honeycomb.

#### Diffuser Loss

Immediately downstream of the test section is the diffuser. The diffuser for a 12 inch tunnel would be 12 inches by 12 inches at the inlet, allowing it to match the test section exit, and 17 inches in diameter at the exit, allowing it to match the fan inlet. The length of the diffuser is 58 inches. The design details of the diffuser may be found in the next chapter.

There seems to be large differences in the value of diffuser losses using different methods for a particular diffuser. One reason for this is that some methods take the effect of entrance and exit length, while others do not. Other differences are usually due to method and the number of parameters used in determining the loss.



Although there seems to be no loss equation specifically for a square-to-round diffuser, a loss coefficient can be determined with the help of several references. Assigning the subscripts "1" and "2" to the inlet and exit conditions, respectively, of the diffuser, the energy equation in a simplified form is

$$P_1 + \rho V_1^2/2 = P_2 + \rho V_2^2/2 + \Delta p_d \quad (11)$$

where  $\Delta p_d$  is the effective total pressure loss through the diffuser, including the total pressure loss plus the effect of velocity redistribution caused by the diffuser[4]. Substituting the continuity equation into equation (11) gives

$$P_1 + \rho V_1^2/2 = P_2 + \rho V_1^2 (A_1/A_2)^2 + \Delta p_d. \quad (12)$$

Solving equation (12) for  $\Delta p_d$  and rearranging terms leaves

$$\Delta p_d = (P_1 - P_2) + \rho V_1^2 (1 - A_1^2/A_2^2)/2. \quad (13)$$

Next the pressure recovery coefficient may be defined as

$$C_p = (P_2 - P_1) / (\rho V_1^2/2)$$

which may be substituted into equation (13) giving

$$\Delta p_d = (-C_p \rho V_1^2/2) + \rho V_1^2 (1 - A_1^2/A_2^2)/2$$

or

$$\Delta p_d = (\rho V_1^2/2) [(1 - A_1^2/A_2^2) - C_p]. \quad (14)$$

Defining the coefficient of loss in the diffuser as

$$K = \Delta p_d / q_d = \Delta p_d / (\rho \bar{V}^2/2) = \Delta p_d / \rho [(V_2 + V_1)/2]^2/2,$$

where  $\bar{V}$  is the average between the inlet and outlet velocities, makes the coefficient of loss with respect to the working section,

$$K_o = \{\Delta p_d / \rho [(V_2 + V_1)/2]^2\} \{[(V_1 + V_2)/2]^2 / V_o^2\} = \Delta p_d / (\rho V_o^2/2). \quad (15)$$

If equation (14) is substituted into equation (15) the result is

$$K_o = [(1 - A_1^2/A_2^2) - C_p] V_1^2 / V_o^2. \quad (16)$$

Although the coefficient of loss of a particular diffuser may be found if the pressure recovery coefficient has been measured, most sources measure the effectiveness of diffusers in terms of an efficiency of energy transformation,  $\eta$ , where

$$\eta = (p_2 - p_1) / (\rho V_1^2 / 2) (1 - A_1^2 / A_2^2) = C_p / (1 - A_1^2 / A_2^2). \quad (17)$$

Substituting equation (17) into equation (16) gives

$$K_o = (1 - A_1^2 / A_2^2) (1 - \eta). \quad (18)$$

The efficiency,  $\eta$ , is determined primarily as a function of the total cone angle of the diffuser. In this case the total cone angle would be

$$2\theta = 2 \tan^{-1} [(D_{e2} - D_{e1}) / 2L_d] = 2 \tan^{-1} [(17-12) / 2 \cdot 58] = 5.0^\circ$$

where  $2\theta$  is the total cone angle,  $D_{e2}$  is the effective diameter at the diffuser exit,  $D_{e1}$  is the effective diameter at the diffuser inlet, and  $L_d$  is the length of the diffuser.

With a  $5.0^\circ$  total cone angle Cockrell and Markland[5] give  $1-\eta$  a value of approximately 0.15 for this type of flow, where  $1-\eta$  is the pressure loss coefficient,  $\lambda$ . Substituting this value for  $1-\eta$  into equation (18) gives

$$K_o = [1 - (4 \cdot 12^2 / \pi \cdot 17^2)^2] 0.15 = 0.090.$$

#### Second Honeycomb Section Loss

The second honeycomb section is immediately downstream of the diffuser section. Although a tube type honeycomb with length/diameter = 5.0 is the actual honeycomb used in the tunnel, the original design called for a hexagonal honeycomb with a length to diameter ratio of 6.0. Since Pope[2] recommends a  $K$  of 0.20 for a hexagonal honeycomb with length to diameter ratio of 6.0, the loss coefficient,  $K_o$ , becomes

$$K_o = K(A_o / A_h)^2 = 0.20 [1 / \pi (17)^2 / 4 (144)]^2 = 0.080$$

where  $A_h$  is the cross-sectional area of the honeycomb section.

### Fan Exit Loss

The last loss is called the fan exit loss. It is due to the kinetic energy in the air at the exit of the wind tunnel. Since this fan manufacturer and most other manufacturers do not include this in the fan performance data, it must be added to the pressure losses. Thus a loss at least equal to the dynamic head at the fan exit must be added. Stevenson[1] uses a factor of 1.05 times the dynamic head for a value for these losses. Thus

$$K_o = (\Delta P/q)(q/q_o) = 1.05(q/q_o) = 1.05(A_o/A_f)^2 = 1.05(1/1.59)^2 = 0.415$$

where  $A_f$  is equal to  $1.59 \text{ ft}^2$  which is equal to the fan exit area as quoted by the manufacturer.

### Total Loss and Summary

With the energy loss coefficient of each section the Energy Ratio may be found by summing the energy loss coefficients and taking the reciprocal. From Table 1 summation of the energy loss coefficients is found to be 0.673. Taking the reciprocal of 0.673, the Energy Ratio becomes

$$E. R. _t = 1/\Sigma K_o = 1/0.673 = 1.49.$$

The Energy Ratio gives the characteristics of the wind tunnel or energy expending part of the system. To get an idea of where the total system operates, the wind tunnel characteristics are plotted on a graph with the manufacturer's fan characteristics. For the wind tunnel, the total static pressure across the system,  $\Delta P_t$ , is plotted against the flow rate,  $Q = AV = A_o V_o$ . Since

$$K_o = \Delta P/q_o,$$

then

$$\Sigma K_o = \Delta P_t/q_o = \Delta P_t/(\rho A_o V_o^2/2).$$

SECTION:	$K_o$ :
Test Section	0.0630
Contraction Section	0.0135
Settling Chamber	0.000875
First Honeycomb Section	0.0111
Diffuser Section	0.090
Second Honeycomb Section	0.080
Fan Exit	<u>0.415</u>
	$\Sigma K_o = 0.673$

Table 1. Summation of Energy Loss Coefficients

Substituting equation (7) into equation (19) and solving for  $\Delta P_t$ , results in

$$\Delta P_t = (\rho A_o V_o^2 / 2) / E. R._t = (\rho V_o Q / 2) / E. R._t.$$

Thus the total static pressure across the system,  $\Delta P_t$ , for a particular flow rate or velocity may be found if the air density,  $\rho$ , and Energy Ratio,  $E. R._t$ , are known. This is done in Figure 1. The intersection of the two curves represent the operating conditions of the total system.

As Figure 1 indicates, the fan curve and wind tunnel curve intersect at approximately 9200 cfm and -3.6 inches of water pressure. Since the cross-sectional area of the test section is 1 ft<sup>2</sup>, the test section velocity would be approximately

$$(9200 \text{ ft}^3/\text{min})(60 \text{ sec}/\text{min})(1 \text{ ft}^2) = 154 \text{ ft}/\text{sec}$$

which is much greater than the minimum allowable 100 ft/sec. Thus the available fan is capable of providing the minimum allowable test section velocity.

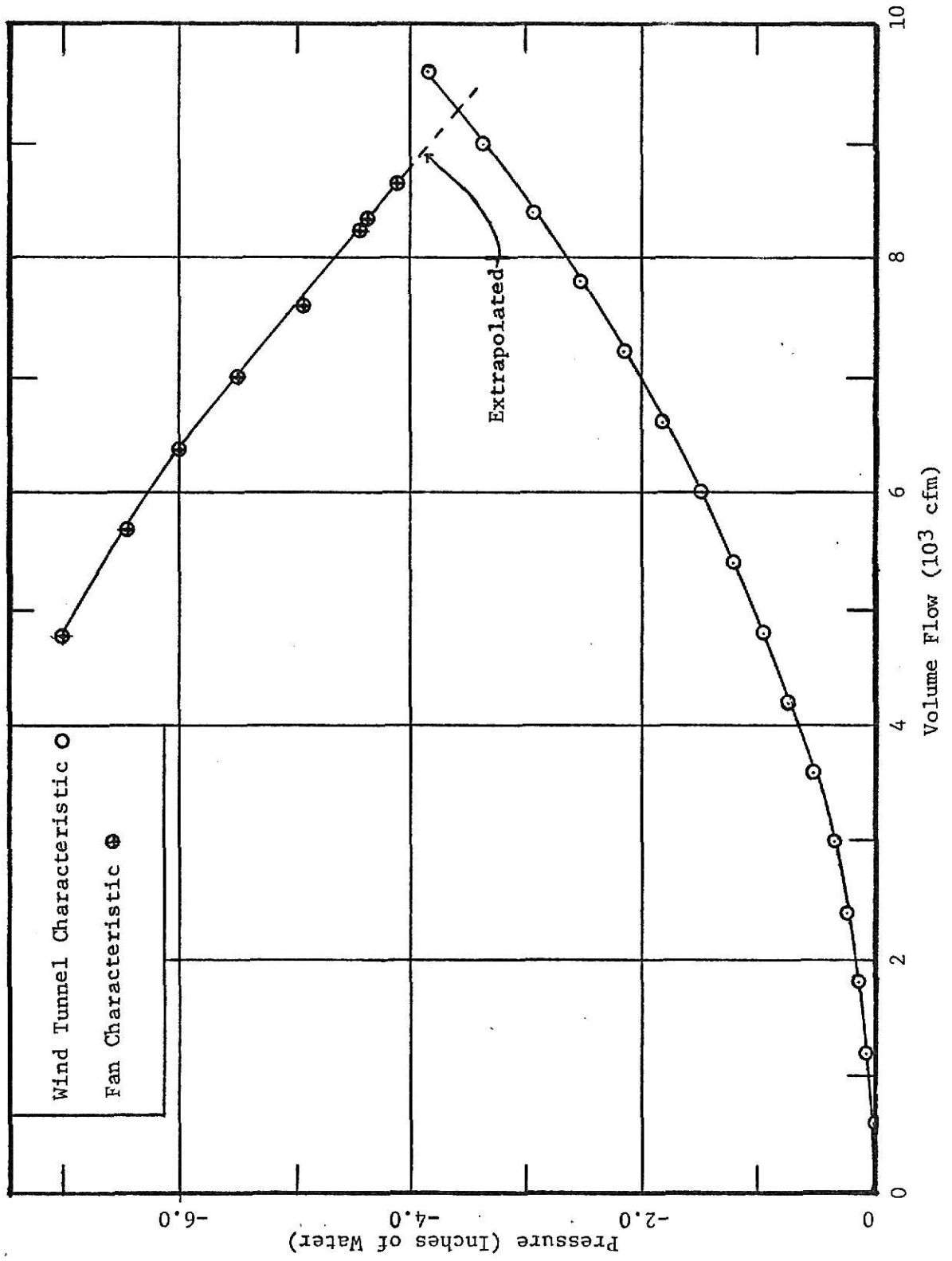


Figure 1. Pressure-Volume Flow for 12 Inch Wind Tunnel and Fan.

## CHAPTER III

### SYSTEM DETAILS

The wind tunnel may be divided into six parts as shown in Figure 2.

They are:

1. The inlet or entry which directs the air into the tunnel.
2. The settling chamber and filter which are designed to reduce velocity variations and turbulence level.
3. The contraction section which provides a uniform stream of air to the test section and reduces the turbulence further.
4. The working or test section.
5. The diffuser which gives pressure recovery before the air enters the fan.
6. The fan and flow regulator.

#### Inlet

The purpose of the inlet is to prevent flow separation at the entry. There is little information available on inlets, but one of the references, D. C. Stevenson[1], suggests a bell mouth entry with the diameter of the bell mouth equal to the width of the tunnel at the entry. This is the type of inlet used. A detailed drawing of the inlet, settling chamber and filter, and contraction sections is shown in Figure 3.

#### Settling Chamber and Filter

The inlet is followed by a 21 inch settling chamber. At the front of the settling chamber is a 1 inch filter made of plastic and rubber coated

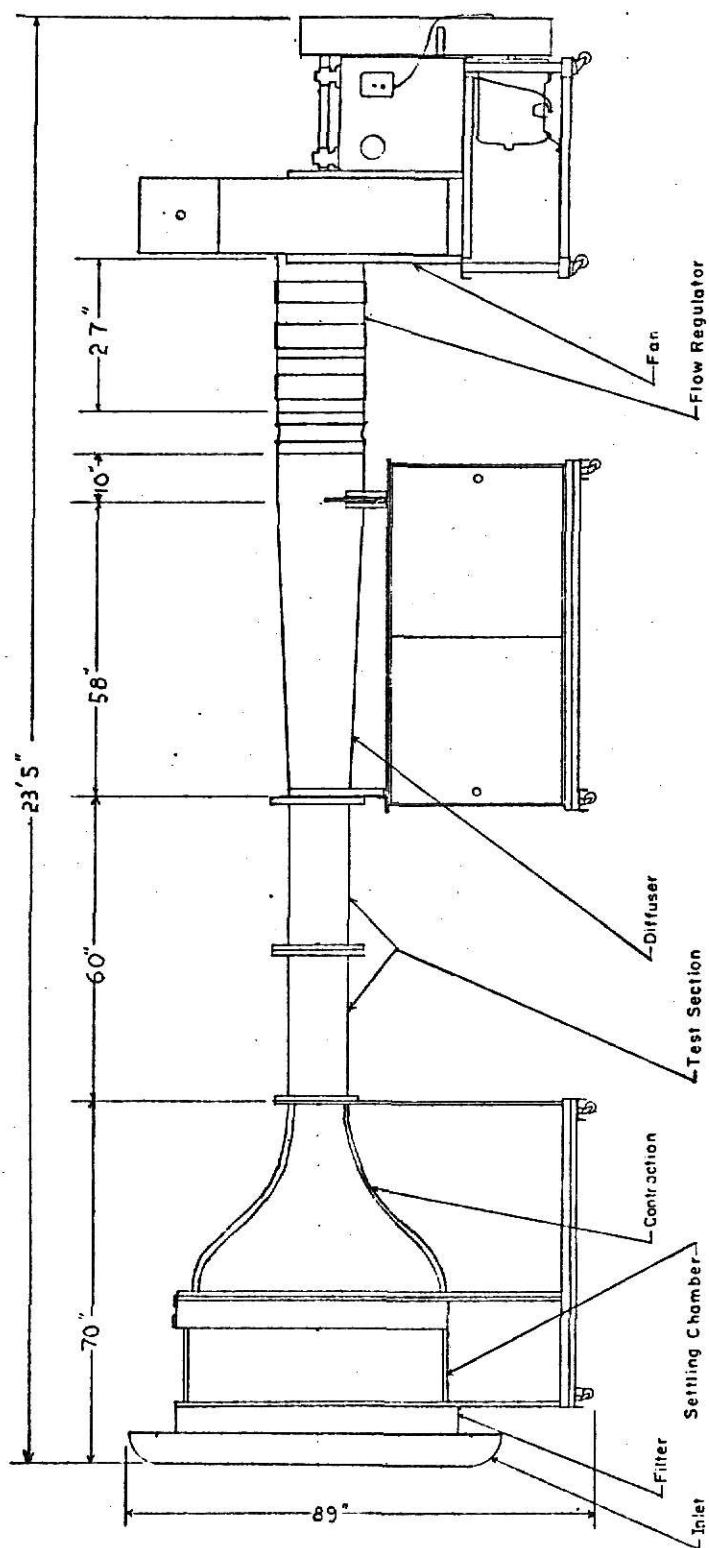


Figure 2. 12 Inch Wind Tunnel.



Section A A  
Without Filter

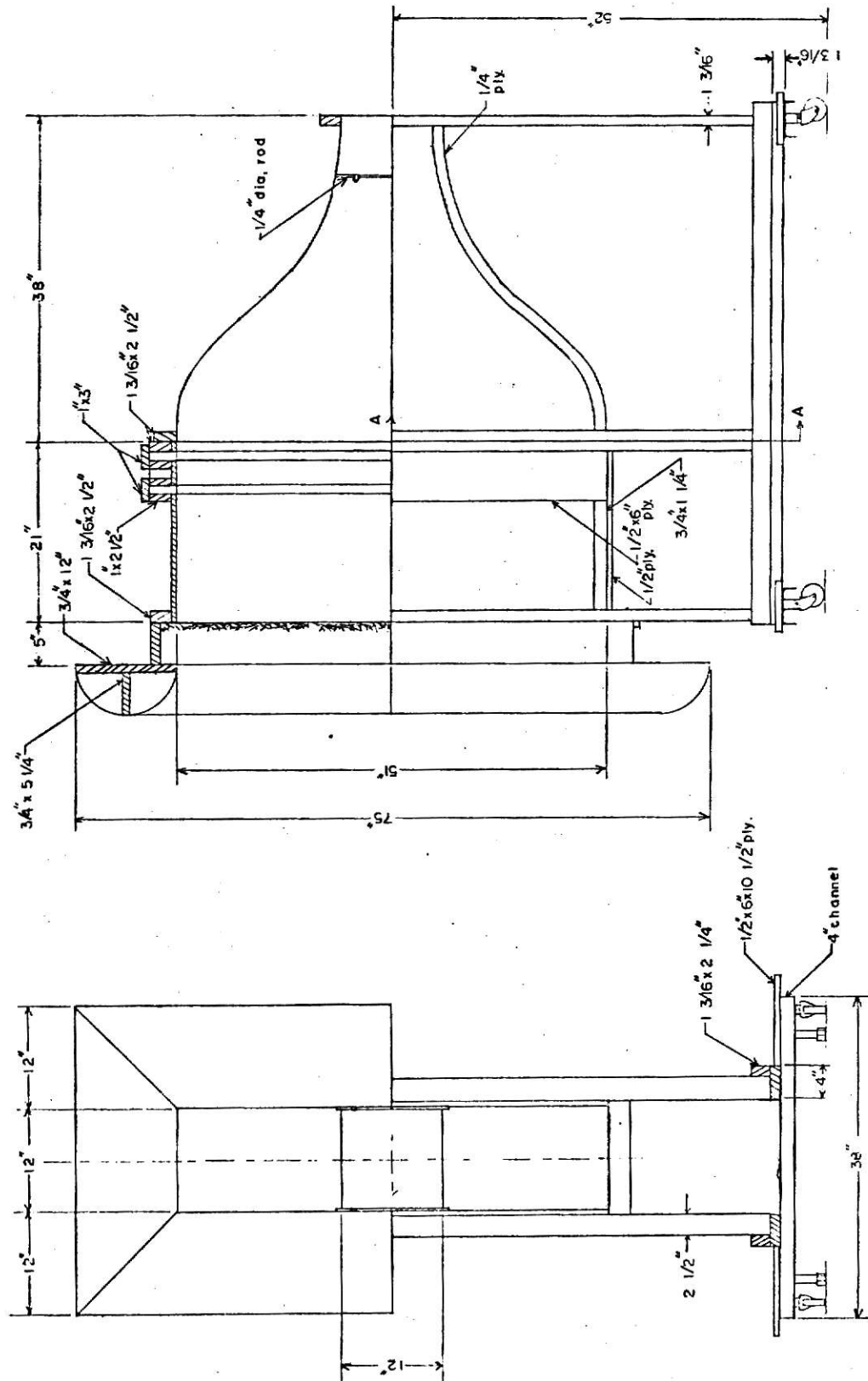


Figure 3. Detail of Inlet, Settling Chamber and Filter, and Contraction Sections.

natural hair which is used to reduce velocity variations and turbulence. The original analysis called for a honeycomb flow straightener. However, it was found that the filter would do the job for approximately \$10 while the honeycomb would cost \$75 to \$100. If there is a need to control the turbulence level further, two 1 inch wide by 1/4 inch deep slots, 15 1/2 inches and 19 1/2 inches from the front of the settling chamber, are provided for more screens. The slots are 4 inches apart to allow for the decay of the turbulence caused by the screens if they were inserted. The period of decay is approximately 500 mesh spacings downstream of the screen[1]. Thus the size of screens will be restricted somewhat to screens with mesh spacings that will allow the turbulence to decay within 4 inches downstream of the first screen.

#### Contraction Section

The contraction section is designed to provide a uniform stream of air, reduce the turbulence, and reduce the flow area while preventing excessive boundary layer build up or separation due to adverse pressure gradients along the walls. Several types of two- or three-dimensional contractions are known to provide an adequate flow condition at the test section. These include contractions with elliptic, cubic or 'nth' order co-ordinates. Stevenson[1] designed a successful two-dimensional contraction for a tunnel of approximately the size and test section velocity as this one. The two-dimensional contraction co-ordinates were obtained by adjusting the contraction co-ordinates of a three-dimensional contraction which was formed by Thwaites'[6] solution of axi-symmetrical flow.

Since Stevenson's contraction has previously been proven satisfactory and because the two-dimensional section is easily constructed, it was used

in almost its exact form for the tunnel of this thesis. It is 38 inches long and has a 51 inch by 12 inch inlet and a 12 inch by 12 inch exit. The only addition is a boundary layer trip on each side of the contraction. Each trip is 13 inches long and is located 7 inches from the small end of the contraction section. A table of the contraction co-ordinates is provided in Table 2.

#### Test Section

The test or working section is actually two 12 inch by 30 inch test sections which may be used together or separately. The sides, top, and bottom of the present test sections are made of 1/2 inch plywood. However, the sections easily come apart, allowing plexiglass sides or an experimental test floor to be installed. As Figure 2 indicates, the test section is supported only at the ends. Thus there are no obstructions that could be in the way of experimental equipment attached to the test section. A detailed drawing of the test section is presented in Figure 4.

#### Diffuser

Since the main purpose of the diffuser is to give pressure recovery before the air enters the fan, the cross-sectional area must increase. However, it should not increase too rapidly or there will be wall separation of the boundary layer causing an energy loss. Neither should it increase too slowly, for if the cone angle of the diffuser is too small, excessive skin friction will cause energy losses. Stevenson[1], Pope[2], and Pankhurst and Holder[7] recommend values of  $5^{\circ}$  to  $7^{\circ}$  total equivalent cone angle as the best compromise between expansion loss and skin friction. The diffuser has a 12 inch by 12 inch inlet and a 17 inch diameter outlet.

X is the horizontal distance in inches from the small end of the contraction section.

Y is the corresponding vertical distance in inches from the centerline of the contraction section.

---

X	Y	X	Y
0	6.0	20.0	13.50
1.0	6.0	21.0	14.55
2.0	6.04	22.0	15.65
3.0	6.10	23.0	16.75
4.0	6.20	24.0	17.90
5.0	6.35	25.0	19.10
6.0	6.50	26.0	20.20
7.0	6.70	27.0	21.30
8.0	6.90	28.0	22.30
9.0	7.18	29.0	23.15
10.0	7.45	30.0	23.80
11.0	7.78	31.0	24.30
12.0	8.26	32.0	24.70
13.0	8.60	33.0	25.00
14.0	9.04	34.0	25.15
15.0	9.57	35.0	25.27
16.0	10.15	36.0	25.32
17.0	10.85	37.0	25.37
18.0	11.67	38.0	25.38
19.0	12.52		

---

Table 2. Contraction Co-ordinates for Two-Dimensional Contraction, Ratio 4.23 to 1.00.

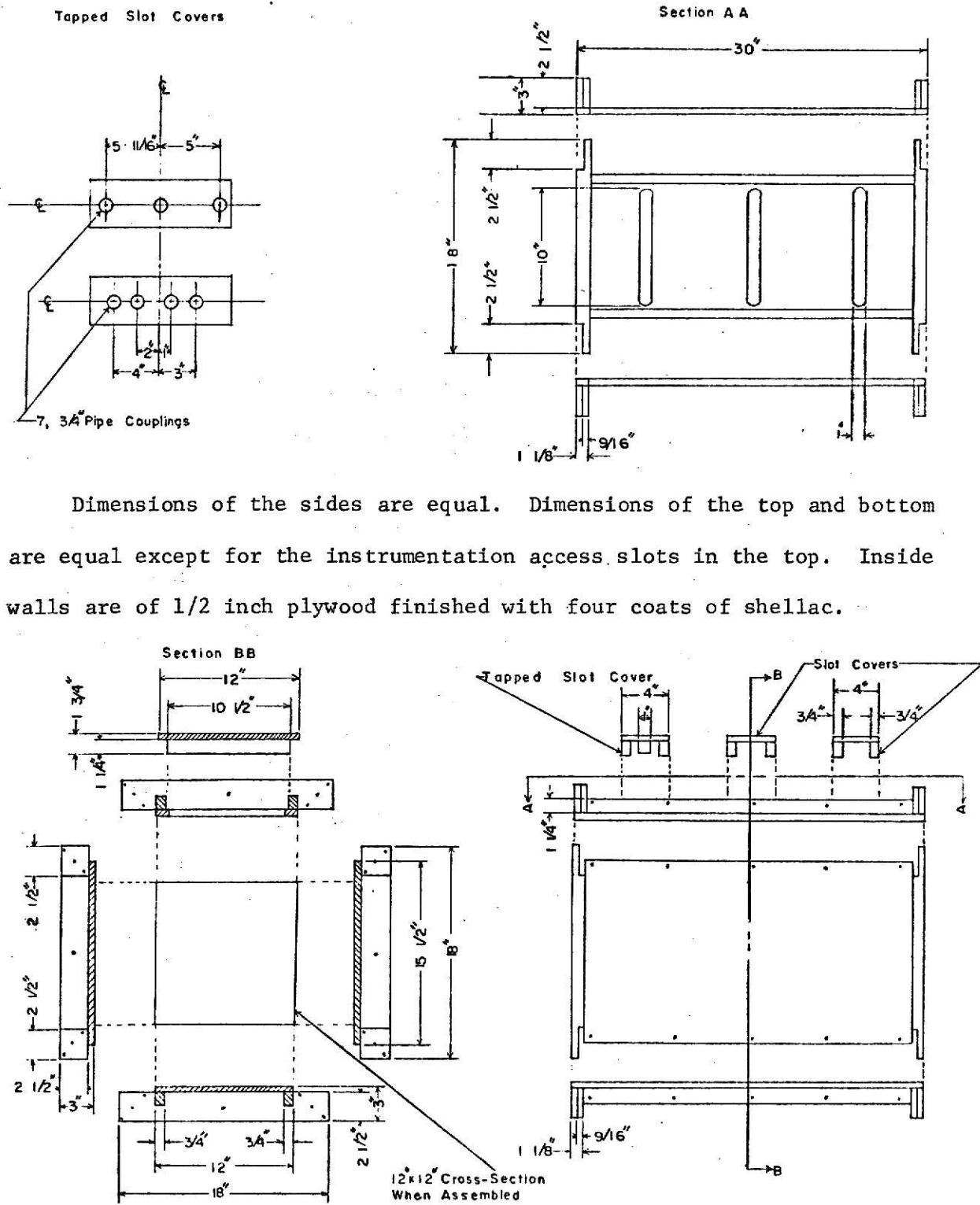


Figure 4. Test Section Detail.

Thus a length of 58 inches was chosen for the length of the diffuser, giving a total equivalent cone angle of  $5^{\circ}$ .

On the downstream end of the diffuser is a 17 inch diameter by 10 inch long cylindrical section which contains a honeycomb of 2 inch diameter by 10 inch long tubes. Although the analysis called for hexagonal honeycombs with a length six times the diameter or width of the honeycombs, the 2 inch by 10 inch tubes were available and no fan swirl was detected in the test section during testing[2].

#### Fan and Flow Regulator

The last section consists of the fan and flow regulator. The fan is a centrifugal type with a 30 inch wheel, 17 inch diameter inlet and 16 5/16 inch by 14 1/2 inch outlet. It is powered by a 10 horsepower motor. The regulator is a 29 inch by 17 inch cylinder with a set of twenty-one 1 inch diameter holes, a set of fifteen 2 inch diameter holes, and a set of four 4 inch by 10 inch and one 4 inch by 3 1/4 inch slots. Three bands about the cylinder slide over the holes to regulate the flow through the wind tunnel. The original design called for a butterfly type regulator at the exit of the fan. However, the butterfly type regulator was found to be unfeasible, and it was decided that a perforated cylinder type flow regulator would allow more accurate regulation of the amount of air flow through the test section.

The regulator and fan are connected to the honeycomb by a flexible canvas connector. The connector helps prevent fan vibration from being transmitted to the rest of the wind tunnel.

## CHAPTER IV

### CHARACTERISTIC RESULTS

For the proposed uses of this tunnel, a uniform velocity in the test section is desired. The velocity should be the same at any station in a cross-section and from station to station in the flow direction. To provide information on velocity uniformity, the test section centerline velocity and cross-sectional velocity profile were measured using a micromanometer and a pitot tube mounted in the instrumentation access slots. With the use of the flow regulator, the velocity profile was measured at stations 7 1/2 inches, 28 1/2 inches, and 46 1/2 inches from the beginning of the test section at maximum and minimum test section velocity, and 7 1/2 inches from the beginning of the test section at a velocity intermediate between the maximum and minimum.

The velocity at a point in the test section is found using the pitot tube-micromanometer arrangement to measure the dynamic pressure at that point. The law of conservation of energy may be written as

$$V_1^2/2g_cJ + P_1/\rho_1J = P_o/\rho_oJ$$

where  $V_1$  is the velocity at point "1",  $P_1$  is the pressure at point "1",  $\rho_1$  is the density of air at point "1",  $P_o$  is the stagnation pressure at point "1", and  $\rho_o$  is the stagnation density of the air at point "1", or

$$V_1^2 = 2(P_o/\rho_oJ - P_1/\rho_1J)g_cJ. \quad (20)$$

Assuming  $\rho_1 = \rho_o = \rho_a$  and calling  $P_o - P_1 = \Delta P$  = the dynamic pressure, equation (20) becomes

$$V_1 = \sqrt{2g_c \Delta P / \rho_a} . \quad (21)$$

From manometry and fluid statics, the dynamic pressure is equal to the specific weight of the water or fluid in the micromanometer multiplied by the height of this fluid, or

$$\Delta P = \rho_w (g/g_c) (h/12) \quad (22)$$

where  $\rho_w$  is the density of water and  $h$  is the height of fluid column in inches. Substituting equation (22) into equation (21) yields

$$V_1 = \sqrt{h \rho_w g / 6 \rho_a} . \quad (23)$$

Assuming the specific weight of water to be  $62.4 \text{ lb/ft}^3$ , equation (23) becomes

$$V_1 = 18.27 \sqrt{h / \rho_a} \quad (24)$$

where  $h$  is in inches of water,  $V_1$  is in ft/sec and  $\rho_a$  is in  $\text{lb}_m/\text{ft}^3$ . (It should be noted that vapor pressure effects are neglected when finding the air density,  $\rho_a$ . Proof that this may be done is found in Appendix A.)

The measured centerline velocity ranges from a minimum of approximately 47 ft/sec at a static pressure of -0.69 inches of water to a maximum of approximately 140 ft/sec at a static pressure of -5.6 inches of water. With the use of the flow regulator, the velocity is continuously variable from the minimum to the maximum. At maximum velocity the centerline velocity ranges from 139 ft/sec 7 1/2 inches from the beginning of the test section to 140 ft/sec 28 1/2 inches from the entrance of the test section to 142 ft/sec 46 1/2 inches from the beginning of the test section. Total variation between 7 1/2 inches to 46 1/2 inches from the beginning of the test section is 2.1%. The 2.1% increase in centerline velocity is due to boundary layer growth along the test section walls and is a small enough



increase for either class laboratory work or research work in convection heat and mass transfer and aerodynamics.

The results of the cross-sectional velocity profiles are shown in Figures 5, 6, 7, 8, 9, 10, and 11. Each point on each figure represents a point at which the static and dynamic pressure were measured. The dynamic pressure was converted to a velocity using equation (24). The velocity at each point was divided by the centerline velocity at that cross-section and multiplied by 100%.

As Figures 5 through 11 show, there is little evidence of a trend in the cross-sectional velocity profile. At 28 1/2 and 46 1/2 inches from the start of the test section (Figures 6 and 7) the left side and especially the left lower portion of the cross-sections tend to have a very smooth profile with a velocity variation of 0.0% to  $\pm 0.5\%$  from the centerline velocity at the maximum test section velocity. As can be verified from Figure 5, even this trend disappears at the maximum velocity condition 7 1/2 inches from the test section entrance, and there exists a fairly uniform profile across the entire cross-section at this point. Although the variation from the centerline velocity is slightly worse at the cross-sections 7 1/2, 28 1/2, and 46 1/2 inches from the start of the test section at the minimum velocity (Figures 8, 9, and 10) and at 7 1/2 inches from the beginning of the test section at the intermediate velocity (Figure 11), there are only two measured points where the velocity was greater than  $\pm 2.0\%$  of the centerline velocity at the cross-section. There does not appear to be any trend at the minimum and intermediate test section velocities 7 1/2 inches from the test section entrance. The trend 28 1/2 and

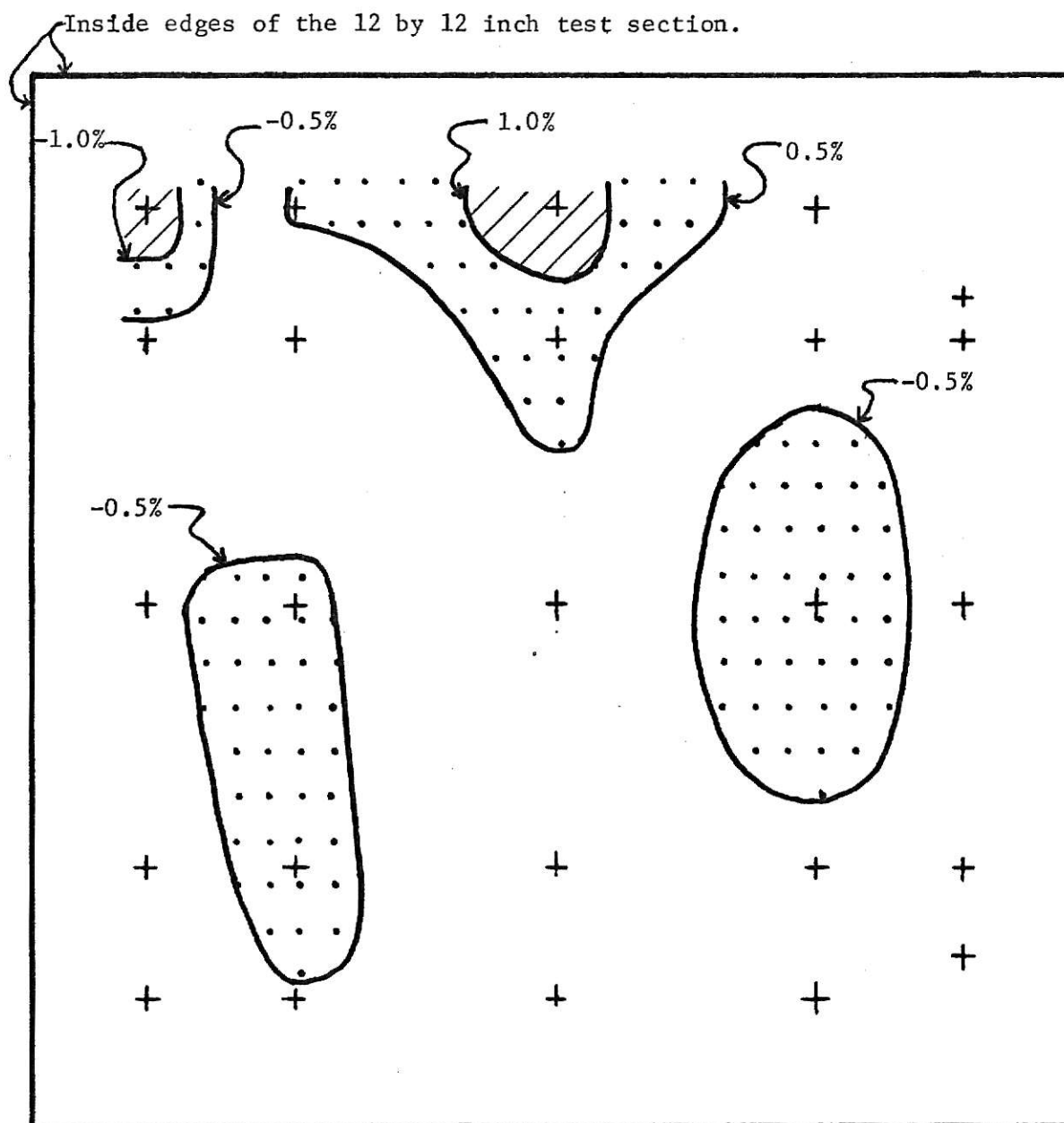
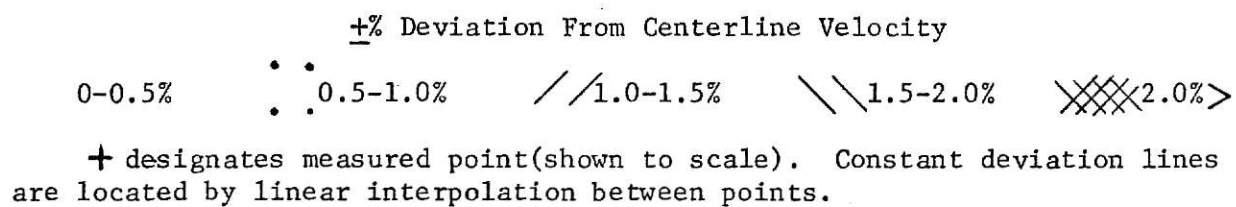


Figure 5. Cross-Sectional Velocity Profile 7 1/2 Inches From Start of Test Section at a Test Section Velocity of 139 ft/sec.

+% Deviation From Centerline Velocity

0-0.5%

• •

• •

0.5-1.0%

1.0-1.5%

1.5-2.0%

~~2.0%~~

+ designates a measured point (shown to scale). Constant deviation lines are located by linear interpolation between points.

Inside edges of the 12 by 12 inch test section.

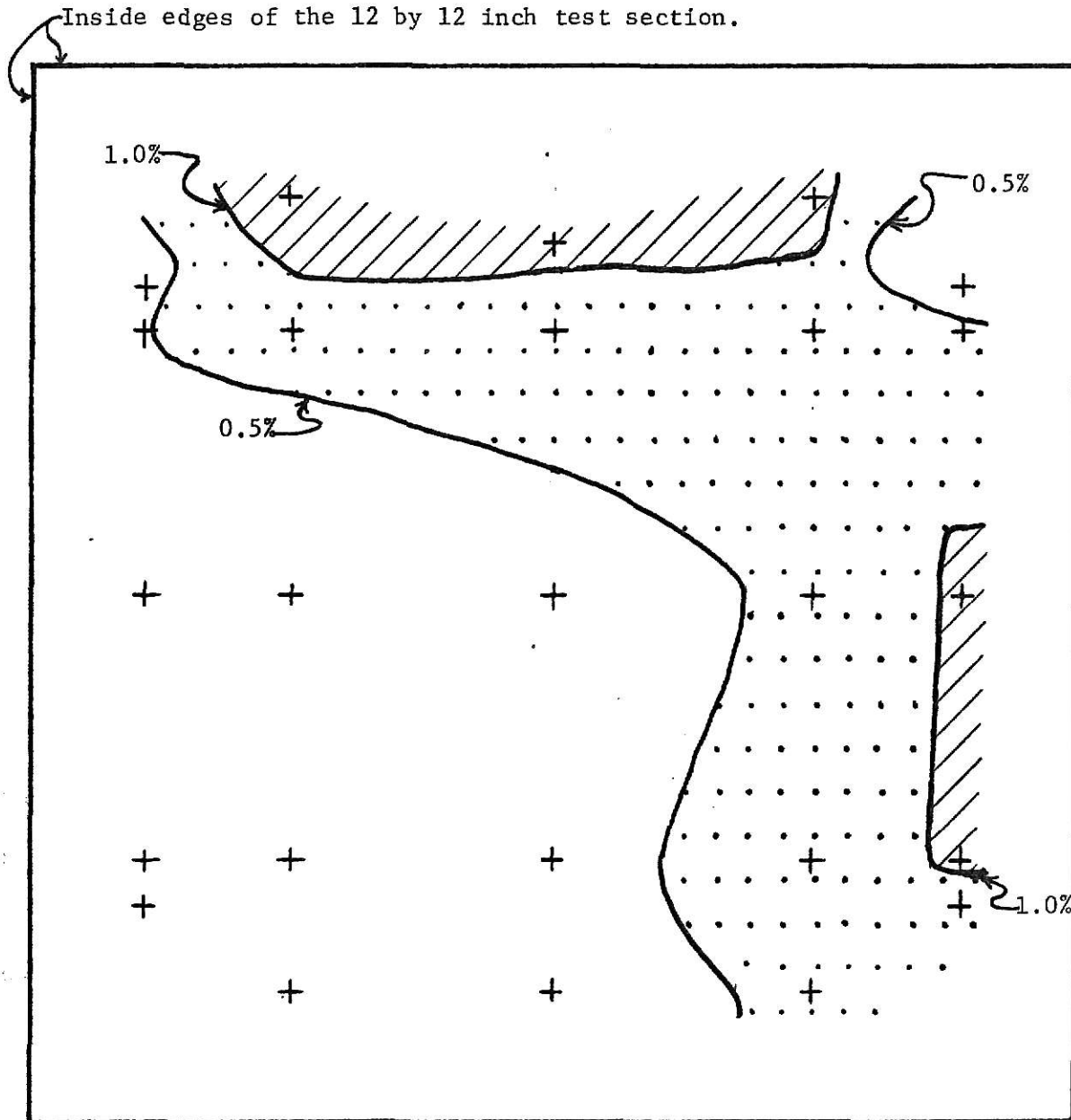


Figure 6. Cross-Sectional Velocity Profile 28 1/2 Inches From Start of Test Section at a Test Section Velocity of 140 ft/sec.



+ % Deviation From Centerline Velocity

0-0.5%    ••• 0.5-1.0%    // 1.0-1.5%    \\\ 1.5-2.0%    XXXX 2.0%>

+ designates a measured point (shown to scale). Constant deviation lines are located by linear interpolation between points.

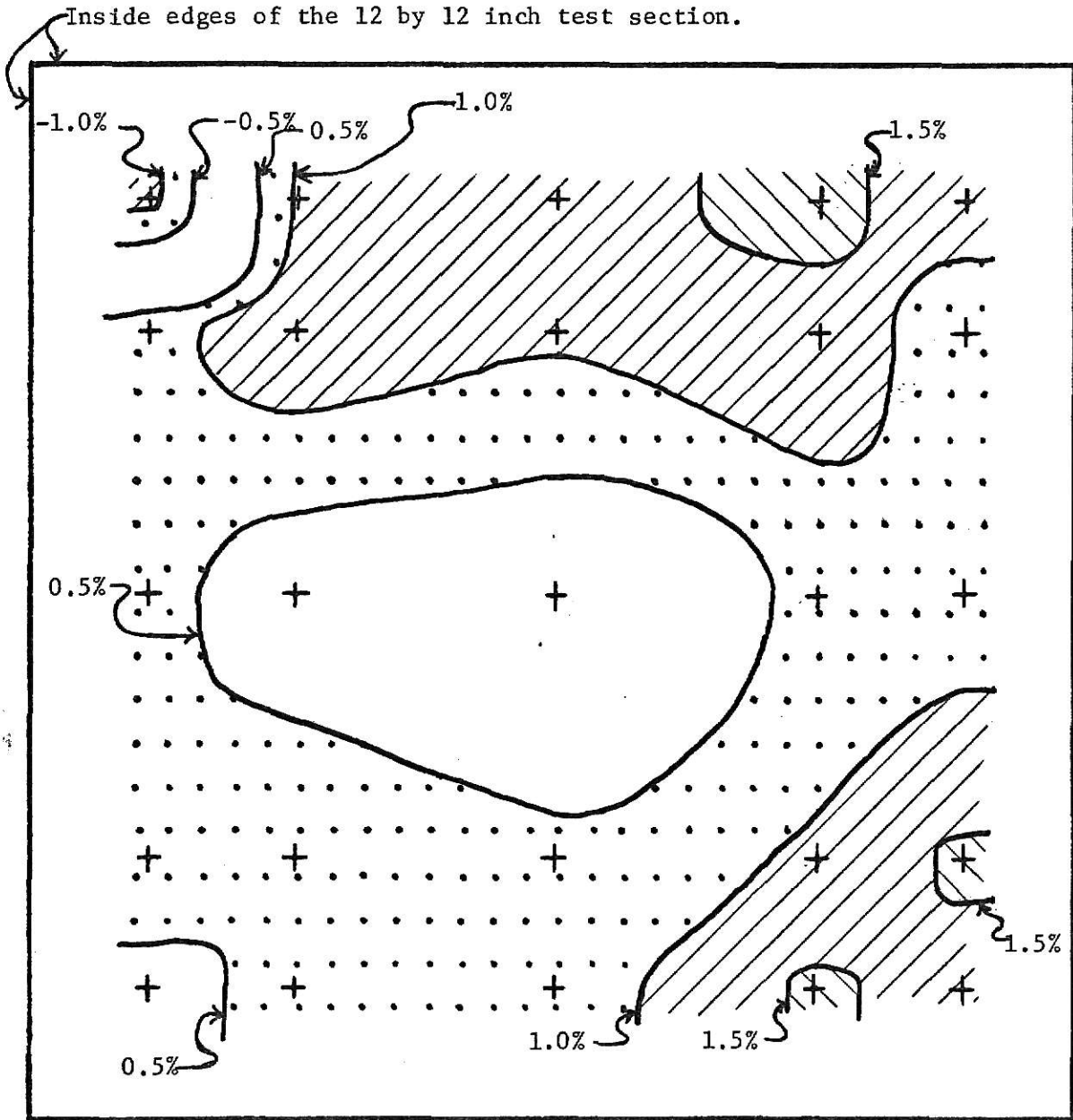


Figure 8. Cross-Sectional Velocity Profile 7 1/2 Inches From Start of Test Section at a Test Section Velocity of 47 ft/sec.

+ % Deviation From Centerline Velocity

0-0.5%    . . . 0.5-1.0%    / / 1.0-1.5%    \ \ 1.5-2.0%    x x x x 2.0% >

+ designates a measured point (shown to scale). Constant deviation lines are located by linear interpolation between points.

Inside edges of the 12 by 12 inch test section.

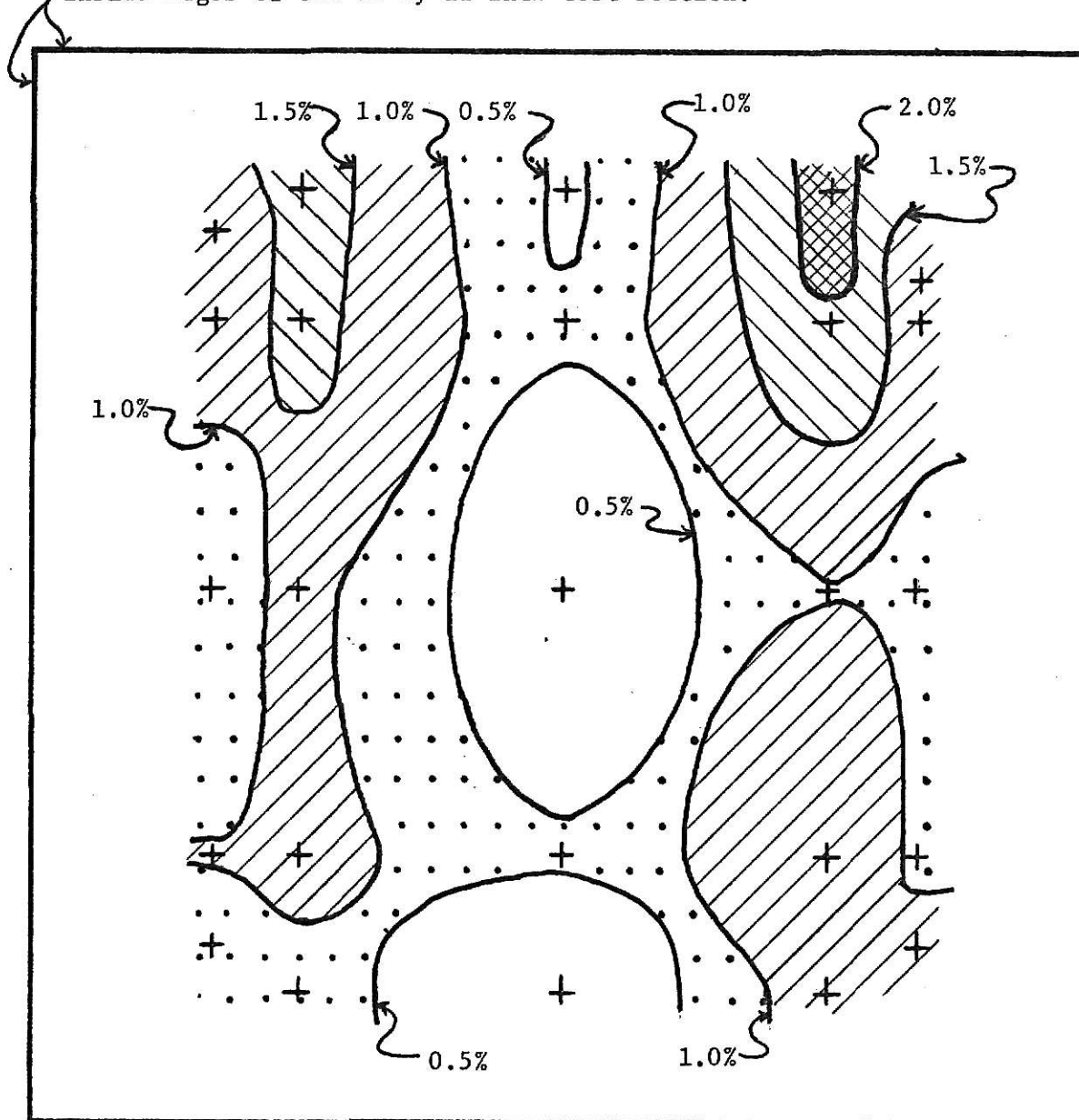



Figure 9. Cross-Sectional Velocity Profile 28 1/2 Inches From Start of Test Section at a Test Section Velocity of 48 ft/sec.

±% Deviation From Centerline Velocity

0-0.5%    ···· 0.5-1.0%    // 1.0-1.5%    \\\ 1.5-2.0%     2.0%>

+ designates a measured point (shown to scale). Constant deviation lines are located by linear interpolation between points.

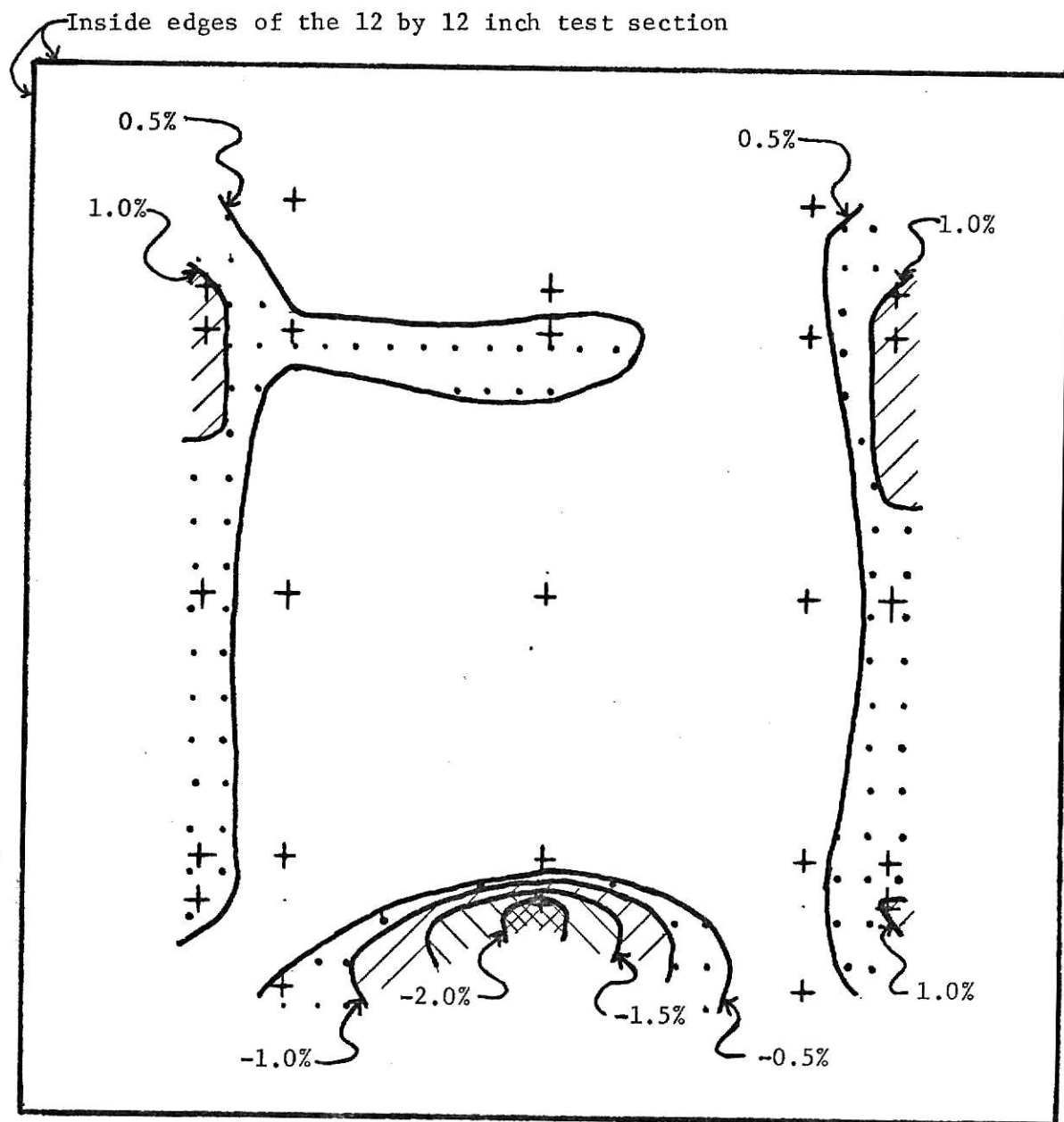


Figure 10. Cross-Sectional Velocity Profile 46 1/2 Inches From Start of Test Section at a Test Section Velocity of 48 ft/sec.

+ % Deviation From Centerline Velocity

0-0.5%	• • 0.5-1.0%	// 1.0-1.5%	\\ 1.5-2.0%	XXXX 2.0% >
--------	--------------	-------------	-------------	-------------

+ designates a measured point (shown to scale). Constant deviation lines are located by linear interpolation between points.

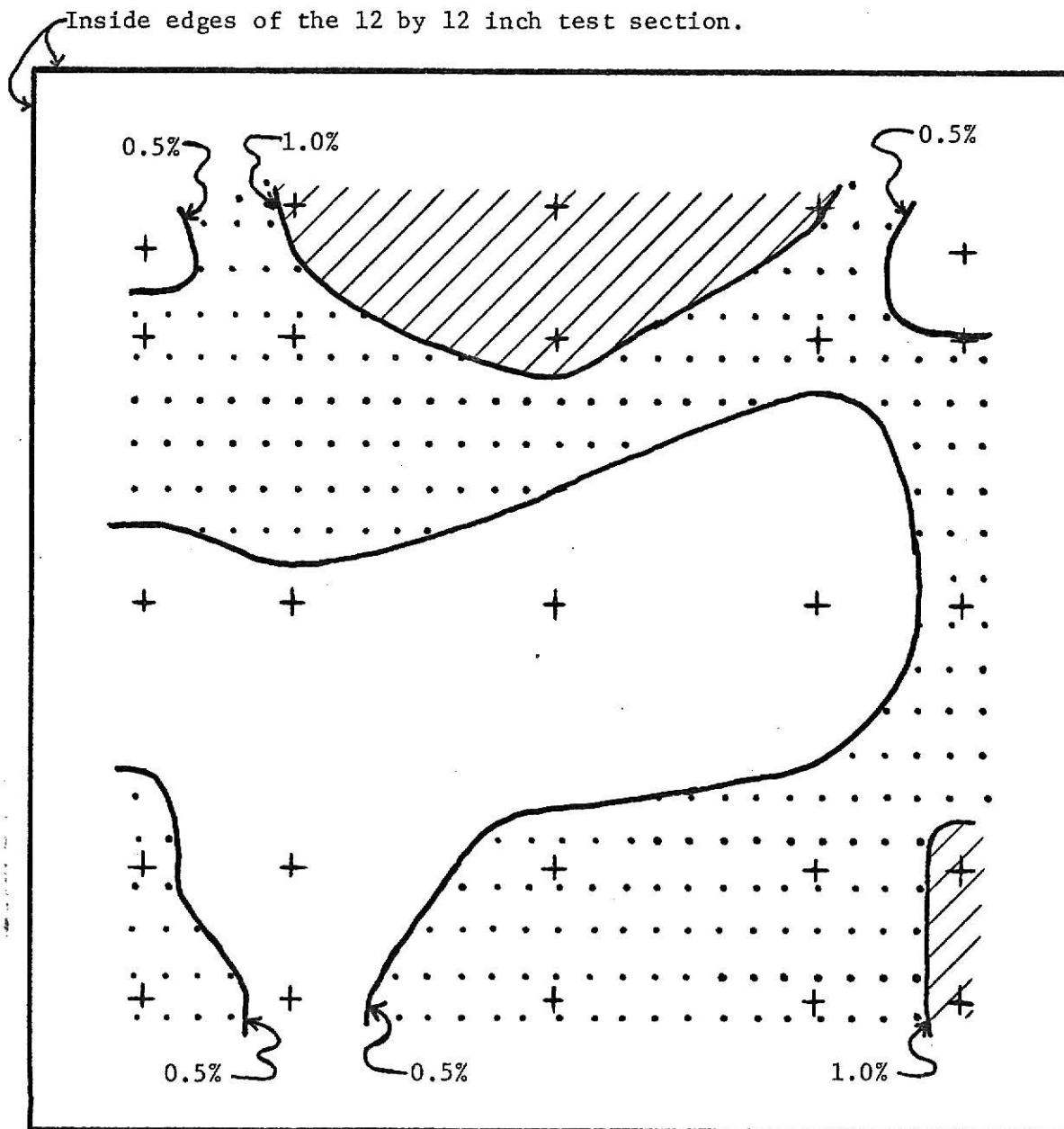


Figure 11. Cross-Sectional Velocity Profile 7 1/2 Inches From Start of Test Section at a Test Section Velocity of 92 ft/sec.



46 1/2 inches from the beginning of the test section at maximum velocity completely disappears at minimum test section velocity.

Thus the test section of the wind tunnel has a sufficiently uniform velocity distribution for either class laboratory work or research work in convection heat and mass transfer and aerodynamics. The velocity profile is within the  $\pm 2.0\%$  variation which is the variation acceptable for these uses.

It should be noted that the outer points of each cross-section are not necessarily at the edge of the boundary layer. They are within a range where the manometer fluid position was stable enough to read to three significant figures. It would not be best to use an aerodynamic model in the test section whose outer edges lie outside the measured points of the cross-section (approximately 7 inches by 7 inches). Figures 5 to 11 show the outer bounds of the measured points. It would be impossible to describe the largest possible model that could be placed in the test section for it would depend on the shape of the model.

In Chapter II, System Analysis, the wind tunnel characteristics curve and the fan performance curve were shown to intersect at approximately 9200 cfm., 154 ft/sec test section velocity, at a pressure of -3.6 inches of water. Measurement of these parameters in the actual tunnel gave a maximum test section velocity of approximately 140 ft/sec at a pressure of approximately -4.2 inches of water. Although there were three primary differences between the actual tunnel and the tunnel in the original analysis, the actual tunnel's characteristics were in close enough agreement with those in the original analysis that the actual 12 inch tunnel provided in excess the minimum test section velocity of 100 ft/sec stated in the introduction.

## CHAPTER V

### SUMMARY

There appears to be no trend of non-uniformity in the cross-sectional velocity profile of the test section. Although at maximum test section velocity the left to left lower corner of the cross-sections 28 1/2 and 46 1/2 inches from the start of the test section is quite flat and within  $\pm 0.5\%$  of the centerline velocity, this trend disappears 7 1/2 inches from the test section origin at maximum, minimum, and intermediate test section velocities.

The velocity variation from the centerline velocity is within  $\pm 2.0\%$  at all but two of the measured points. These two points were at minimum test section velocity and became less than  $\pm 2.0\%$  at the same points at maximum test section velocity. Thus, for the region of measured points, the velocity profile has a velocity variation of less than  $\pm 2.0\%$  at maximum velocity and at all but two points at minimum velocity.

The test section of the wind tunnel has a sufficiently uniform velocity distribution for either class laboratory work or research work in convection heat and mass transfer and aerodynamics.

The velocity range in the test section is continuously variable from 47 ft/sec to a maximum of 140 ft/sec. The size of aerodynamic model that may be inserted in the test section depends upon the geometric shape of the tunnel. However, the model should not extend beyond the measured points of the cross-section (Figures 5 through 11).

#### REFERENCES

1. Stevenson, D. C. "Design and Construction of a Small Wind Tunnel." Bulletin of Mechanical Engineering Education, VIII (January 15, 1968), 11-21.
2. Pope, A. Wind Tunnel Testing. New York: John Wiley & Sons, 1954.
3. Pope, A. and Harper, J. J. Low-Speed Wind Tunnel Testing. New York: John Wiley & Sons, 1966.
4. Reid, E. G. "Performance Characteristics of Plane Wall Two-Dimensional Diffusers." NACA, TN2888, February, 1953.
5. Cockrell, D. J. and Markland, E. "A Review of Incompressible Diffuser Flow." Aircraft Engineering, XXXV (October, 1963), 286-292.
6. Thwaites, B. "On the Design of Contractions for Wind Tunnels." Aeronautical Research Council, Reports & Memoranda No. 2278, March, 1946.
7. Pankhurst, R. C. and Holder, D. W. Wind Tunnel Technique. London: Pitman & Sons, 1952.
8. Jennings, B. H. and Lewis, S. R. Air Conditioning and Refrigeration. Scranton: International Textbook Co., 1944.
9. Holeman, J. P. Experimental Methods for Engineers. New York: McGraw-Hill, 1966.

## A P P E N D I C E S

## APPENDIX A

Proof that the relative humidity can be neglected in the velocity calculations.

To prove that the relative humidity can be neglected in the velocity calculations the worst case(highest relative humidity) should be used. This case would be on February 24, 1970 when the relative humidity at the fan location was approximately 51% and the barometric pressure was 14.19 psia. The wet-bulb temperature was 46.0°F and the dry-bulb temperature was 54.5°F.

From the Carrier equation[8]

$$P_v = P_w - (P_b - P_w)(t_d - t_w)/(2800 - 1.3t_w)$$

where  $P_v$  is the pressure of the water vapor in the atmosphere,  $P_w$  is the pressure of the water vapor at the wet-bulb temperature,  $P_b$  is the barometric pressure,  $t_d$  is the dry-bulb temperature, and  $t_w$  is the wet-bulb temperature(°F), the water vapor pressure would be

$$P_v = 0.15323 \text{ lb/in}^2 - \frac{(14.19 \text{ lb/in}^2 - 0.15323 \text{ lb/in}^2)(54.5^\circ\text{F} - 46.0^\circ\text{F})}{2800 - 1.3(46.0^\circ\text{F})}$$

$$= 0.1077 \text{ lb/in}^2$$

where 0.15323 lb/in<sup>2</sup> is the saturated vapor pressure. Since the vapor pressure is 0.1077 lb/in<sup>2</sup>, the pressure of dry air would be

$$P_{da} = P_b - P_v = 14.19 - 0.1077 = 14.08 \text{ lb/in}^2$$

where  $P_{da}$  is the dry air partial pressure.

Knowing the dry air and water vapor partial pressures, the mass of dry air per unit volume and the mass of water vapor per unit volume may be found. The mass of dry air per unit volume would be

$$m_{da}/V = P_{da}/R_{da}T_d = (14.08)(144)/(53.34)(514.5) = 0.07392 \text{ lb}_m/\text{ft}^3$$

where  $m_{da}/V$  is the mass of dry air per unit volume,  $R_{da}$  is the gas constant for dry air, and  $T_d$  is the dry bulb temperature(°R). The mass of water vapor per unit volume would be

$$m_v/V = P_v/R_v T_d = (0.1077)(144)/(85.76)(514.5) = 0.0003515 \text{ lb}_m/\text{ft}^3$$

where  $m_v$  is the mass of water vapor per unit volume and  $R_v$  is the gas constant for water vapor. Thus the total mass per unit volume is

$$m_{da}/V + m_v/V = 0.07427 \text{ lb}_m/\text{ft}^3 = \rho_{a1}$$

where  $\rho_{a1}$  is the fluid density with the effect of the relative humidity included.

However, if the fluid density is calculated using the ideal gas law and assuming that the gas constant,  $R$ , is equal to the gas constant for dry air, the fluid density becomes

$$\rho_{a2} = P_b/R_{da} T_d = (14.19)(144)/(53.34)(514.5) = 0.07448 \text{ lb}_m/\text{ft}^3.$$

The velocity variation due to using the ideal gas law and the dry air gas constant rather than calculating the effect of the relative humidity would be

$$\begin{aligned} \Delta V &= (100\%)(V_{a1} - V_{a2}) \\ &= (100\%)(18.27\sqrt{h/\rho_{a1}} - 18.27\sqrt{h/\rho_{a2}})/(18.27\sqrt{h/\rho_{a1}}) \end{aligned} \quad (25)$$

where  $\Delta V$  is the velocity variation,  $V_{a1}$  is the velocity using  $\rho_{a1}$ ,  $V_{a2}$  is the velocity using  $\rho_{a2}$ , and  $h$  is the water column height. The water column height would be a constant; thus, simplifying, equation (25) would become

$$\Delta V = (1 - \rho_{a1}/\rho_{a2})100\%. \quad (26)$$

Substituting into equation (26) yields

$$\Delta V = (1 - 0.07427/0.07448)100\% = 0.14\%.$$

Thus the ideal gas law using the dry air gas constant would produce a maximum error of 0.14%. With an allowable velocity variation from the centerline velocity of approximately 2%, the 0.14% maximum error would be less than 1/10 the allowable velocity variation. Thus the effect of the relative humidity can be neglected.

## APPENDIX B

### ERROR ANALYSIS

To establish the accuracy of the experimental results, an error analysis was made. Let  $\Delta V$  be the uncertainty in the result and  $\Delta \rho$  and  $\Delta h$  be the uncertainties in the independent variables in the equation, then

$$V = 18.27\sqrt{h/\rho},$$

where  $h$  is the manometer water column height in inches of water,  $\rho$  is the air density in  $\text{lb}_m/\text{ft}^3$ , and  $V$  is the flowing air velocity in  $\text{ft}/\text{sec}$ . Then the uncertainty in the result is

$$\Delta V = \{[(\partial V/\partial h)\Delta h]^2 + [(\partial V/\partial \rho)\Delta \rho]^2\}^{1/2} \quad [9]. \quad (27)$$

Using the conditions on the day of maximum humidity and assuming minimum velocity (minimum velocity readings were being taken that day), a typical  $h$  was  $h = 0.520$  inches of water  $\pm 2.0\%$  and the density was  $0.07427 \text{ lb}_m/\text{ft}^3$  with an uncertainty of less than  $\pm 1\%$  (the determination of  $\Delta \rho$  was done in the same manner as  $\Delta V$  is being determined). Since

$$\partial V/\partial h = 9.13/\sqrt{h\rho}$$

and

$$\partial V/\partial \rho = -9.13/\sqrt{h\rho^3}$$

then

$$(\partial V/\partial h)\Delta h = 9.13(0.02)(0.520)/\sqrt{(0.520)(0.07427)} = 0.483$$

and

$$(\partial V/\partial \rho)\Delta \rho = -9.13(0.01)(0.07427)/\sqrt{0.520(0.7427)^3} = -0.465$$

where  $\Delta \rho = \pm 1\%$ .



Substituting these two values into equation (27) gives

$$v = [(0.483)^2 + (-0.465)^2]^{1/2} = 0.212 \text{ ft/sec.}$$

Thus the error in the velocity is 0.212 ft/sec, which is equivalent to

$$(\Delta v/v)100\% = [(0.212 \text{ ft/sec})/(18.27\sqrt{0.520/0.7448})]100\% = 0.44\%.$$

## ACKNOWLEDGEMENTS

I would like to express my appreciation to Dr. R. L. Gorton for his help and guidance in the work that I did for this thesis and for his great assistance in preparation of the thesis. I would also like to thank Neil Weybrew for his help in construction and on the job design ideas. Neil's contribution to the project is very much appreciated.

Appreciation is expressed to other faculty members who gave advice and assistance, and special acknowledgement goes to my wife for the typing of this thesis.

VITA

William L. Lewis

Candidate for the Degree of  
Master of Science

Thesis: DESIGN, CONSTRUCTION, AND CALIBRATION OF A SMALL SUBSONIC WIND TUNNEL

Major Field: Mechanical Engineering

Biographical:

Personal Data: Born in Council Grove, Kansas, March 15, 1947, the son of William H. and Clela V. Lewis.

Education: Attended grade school in Centralia, Kansas; graduated from Centralia Rural High School, Centralia, Kansas in 1965; attended Kansas State University, Manhattan, Kansas from September, 1965 to October, 1970; received a Bachelor of Science degree in Mechanical Engineering from Kansas State University, Manhattan, Kansas in August 1969; completed requirements for Master of Science degree in Mechanical Engineering in October 1970.

Professional experience: Was employed by the Mechanical Engineering Department at Kansas State University, Manhattan, Kansas during the summer of 1969.

DESIGN, CONSTRUCTION, AND CALIBRATION  
OF A SMALL SUBSONIC WIND TUNNEL

by

WILLIAM LEE LEWIS

B. S., Kansas State University, 1969

---

AN ABSTRACT OF A THESIS

submitted in partial fulfillment of the  
requirements for the degree

MASTER OF SCIENCE

Department of Mechanical Engineering

KANSAS STATE UNIVERSITY  
Manhattan, Kansas

1970

## ABSTRACT

The purpose of this project was to design, build, and test a small subsonic wind tunnel with a test section velocity of at least 100 ft/sec, to include a test section of sufficient size that conveniently sized experiments may be carried out, and to have a cross-sectional velocity variation of no more than  $\pm 2.0\%$  from the centerline velocity.

After researching it was found that to match a given test section and test section velocity to a particular fan, an energy loss across the wind tunnel must be made. This energy loss across the wind tunnel is compared to the characteristic fan curve to find out if the fan is capable of producing the stated test section velocity for the particular size test section. A test section 12 inches square and 60 inches long was decided to be of appropriate size.

One way to find the energy loss is to find the loss in each section of the wind tunnel, relate it to the test section, and add the total to get the total energy loss coefficient. The total energy loss coefficient is equal to

$$K_o = 1/E. R._t = \Delta P_t / (\rho V^2 / 2)$$

where  $E. R._t$  is the Energy Ratio,  $\Delta P_t$  is the total pressure loss through the tunnel and is the required fan pressure,  $\rho$  is the air density, and  $V$  is the test section velocity.

The pressure-volume flow curve for the wind tunnel and the pressure-volume flow curve for the fan were put on a pressure-volume flow graph.

The intersection of the two curves gives the volume flow and thus the test section velocity. The pressure volume curve for the 12 inch square test section in the original analysis intersected the fan curve at approximately -3.6 inches of water pressure and 154 ft/sec(9200 cfm). Thus the available fan is capable of producing over 100 ft/sec through the 12 inch tunnel in the analysis.

The actual tunnel was built using proven designs as much as possible and proven design procedures for the remainder. The wind tunnel may be divided into six parts. The first part or section is the inlet which directs the air into the tunnel. The inlet is attached to the settling chamber and filter which are designed to reduce velocity variations and turbulence level. Immediately downstream of the chamber and filter is the two-dimensional contraction which provides a uniform stream of air to the test section and reduces the turbulence further. The working or test section follows the contraction while the diffuser follows the test section. The diffuser gives pressure recovery before the air enters the fan. The last part of the system is the fan and flow regulator.

The velocity profile was measured using a pitot tube and micromanometer arrangement. The profile was measured 7 1/2, 28 1/2, and 46 1/2 inches from the beginning of the test section at maximum and minimum test section velocities and 7 1/2 inches from the start of the test section at a velocity intermediate between the two.

The test section velocity ranged from a minimum of approximately 47 ft/sec to a maximum of approximately 140 ft/sec. At maximum velocity the centerline test section velocity varied from 139 ft/sec 7 1/2 inches

from the beginning of the test section to 142 ft/sec 46 1/2 inches from the start of the test section.

There appears to be little evidence of a continuing trend in the cross-sectional velocity profile. Except for two points, the variation from the centerline velocity is less than  $\pm 2.0\%$  at all velocities and cross-sections. Thus the stipulation that the test section velocity not vary more than  $\pm 2.0\%$  from the centerline velocity is satisfactorily satisfied.